

Effect of fatty acids on the interfacial and solution behaviour of mixed lipidic aggregates called solid lipid nanoparticles

Abstract

Mutual miscibility of soy lecithin (SLC), tristearin (TS), fatty acids (FA) and curcumin were assessed from surface pressure (π) – area (A) isotherms at air-solution interface with the intention to formulate modified solid lipid nanoparticles (SLN). Appearance of minima in excess area (A_{ex}) and changes in the free energy of mixing (ΔG_{ex}^0) were recorded for systems with 20 mole% FA. Modified SLNs, with potential as topical drug delivery systems, were formulated using the lipids in combination with curcumin, stabilized by aqueous Tween 60 solution. Optimum formulations were assessed by judiciously varying the FA chain length and composition. Physicochemistry of SLNs were investigated by analyzing its size, zeta potential (dynamic light scattering, DLS), morphology (FF-TEM) and thermal behavior (differential scanning calorimetry (DSC)). Size and zeta potential of the formulations were in the range of 300 – 500 nm and -10 to - 20 mV respectively. Absorption and emission spectroscopic studies further support the DLS and DSC observations to confirm the location of curcumin in the palisade layer of SLNs. SLNs sustained the release of incorporated curcumin. Curcumin loaded SLNs showed positive response to gram positive bacteria, *Bacillus amyloliquefaciens*. Combined studies on the physicochemistry of curcumin loaded SLNs, sustained release and antibacterial activity put them forward as promising topical drug delivery agents.

J. Oleo Sci. 2016, 65, 419-430.

1. Introduction

Among the different nanocolloidal drug delivery systems, lipids are superior for its biocompatibility, ease of storage, targeted delivery and control over the release process, *etc*^{1, 2}. Apart from micelles, microemulsions, liposomes, cubosomes and hexosomes,³⁻⁸ the other lipid carriers are solid lipid nanoparticle (SLN) and modified SLN, also known as second generation nanolipid carrier^{1, 9}. SLNs are formulated by replacing oil of the O/W emulsion by solid lipids which have the average diameter of 50-1000 nm. In case of modified SLNs, systems have distinct multicrystalline internal morphology as they are made up of structurally different lipids (solid-solid or solid-liquid). Second generation SLNs thus exhibit superiority over the other delivery systems and have emerged as promising alternates^{1, 10}. Reduced drug expulsion, enhanced drug incorporation efficiency, prolonged physical stability and easy production of second generation SLNs have made them promising drug delivery systems¹¹. Detailed study on the physicochemical characterization and application on different routes of drug administration using SLNs have been well documented in the literature². However, in case of second generation SLNs, the reports are sparse and the works on the physicochemical characterization especially on the long term stability are fragmented in nature. Thus systematic investigations on suitable lipid blends, physicochemical stability and drug payload of modified SLNs are considered to be important.

Selection of appropriate blend of lipids is essential in obtaining a stable SLN dispersion. Although there are no strict thumb rules, however, the usual components of the SLNs include fatty acids, monoglycerides, diglycerides, triglycerides, waxes, liquid lipids, as well as ionic lipids¹². Although the wax based SLNs are more stable, however, they suffer from the major limitations like crystalline modification and drug expulsion during storage, *etc*¹³. Recently our research group has reported stable SLNs whereby the waxy material has been replaced by an unsaturated phospholipid, soy lecithin^{14, 15}. In another report of Wong *et al.*,¹⁶ it was proposed that longer chain fatty acids can undergo slower crystallization compared to the short chain analogs. However, no report on the systematic investigation involving a series of fatty acids are available in literature whereby also the waxy material has been replaced by an unsaturated/oily phospholipid. The present study endeavors to the challenge in understanding the combined effect

of the variation in the concentration and chain length of fatty acid with enhanced physicochemical stability and superior drug payload.

Curcumin, commonly known as turmeric, is a low molecular weight polyphenolic natural product. It has good antioxidant property with a broad spectrum of biological applications: treatment of inflammatory disorder, cancer, HIV infections, cystic fibrosis and Alzheimer, *etc*¹⁷⁻¹⁹. In spite of its wide range of applications, its limited aqueous solubility and low bioavailability restricts its use as a potential drug. Suitable delivery systems are thus warranted to enhance its bioavailability. SLN and liposomes can play major roles in this regard¹⁹⁻²³. However, reports on the use of modified SLNs as carrier for curcumin are limited²⁴. Hence the long term stability of curcumin loaded in modified SLNs and its release study are considered to be very interesting exploratory facets²¹. Due to the presence of chromophoric group, curcumin exhibits strong absorption and emission spectra in the UV-visible region. Polarity dependent shift in the absorption and emission spectra of curcumin can be used to assess the state of polarity and rigidity of SLNs without the need of an additional molecular probe.

Lipidic monolayer at the air-solution interface can simulate the experimentally observed interaction between lipid molecules in the self-aggregated assemblies and similar concept can be extended to mixture of lipids. In order to congruent this issue studies on the interfacial behaviour of the components, being used in formulating the SLNs, are considered to be significant. Mutual miscibility among the components at the air-solution interface can simply be assessed by analyzing the surface pressure (π) – area (A) isotherms. Such studies can also help in understanding the packing behavior of the hydrocarbon chains, which subsequently influences the formation and stability of the aggregated species in the form of SLN.

In the present manuscript, a series of modified SLNs comprising soy lecithin (SLC), tristearin (TS) and fatty acid (FA) were formulated and characterized with special emphasis on the effect of FA concentration and chain length (C12 - C18). Studies on the monomolecular films of the lipids in different molar ratio were performed to assess the optimum lipid composition (miscibility) in preparing SLNs. Curcumin, as a potential drug, were incorporated into the studied systems to evaluate the interaction and associated thermodynamics of the mixed monolayer. Characterizations of the formulated SLNs were subsequently carried out by analysing its size, zeta potential and thermal behavior. FF-TEM studies were performed to obtain the morphological information. Curcumin loaded SLNs were further subjected to absorption and

emission spectroscopy, fluorescence anisotropy, encapsulation, release and antibacterial activity studies. It is believed that such a comprehensive set of studies would help in understanding the role of the FAs in developing a promising drug delivery system for curcumin.

2. Materials and Method

2.1. Materials

Soylecithin ([1,3-bis(sn-3'-phosphatidyl)-sn-glycero]-phosphocholine) was purchased from CALBIOCHEM, Germany. The phospholipid contains linoleic acid (62 - 65%) and palmitic acid (15 - 17%) as stated by the manufacturer. Tristearin (TS) and curcumin [1,7-bis(4-hydroxy-3-methoxyphenyl)-6-heptadiene-3,5-dione] were purchased from Sigma-Aldrich Chemicals, USA. Lauric acid (LA), myristic acid (MA), palmitic acid (PA), stearic acid (SA) and the nonionic surfactant Tween 60, all of analytical grade, were purchased from Sisco Research Laboratory, India. All the chemicals were stated to be >99.5% pure and were used as received. HPLC grade solvents from E. Merck, Mumbai, India were used. Double distilled water with specific conductance of 2-4 μS (at 25 °C) was used throughout the experiment.

2.2. Preparation of SLNs

SLNs were prepared using the standard hot homogenization followed by ultrasonication technique.^{14, 24} Further details are available in our recent publication^{14, 15}. SLN suspensions were stored at 4 °C in dark. In all the formulations total lipid concentration was kept fixed at 1 mM where SLC and TS were used in equimolar ratio. FA proportion/content was varied in the range of 5 – 30 mole % (with respect to total lipid) with an increment of 5 mole%. In case of curcumin loaded SLNs, 20 mole% of FA was used.

2.3. Instrumentation

Langmuir surface balance (Micro Trough X, Kibron, Finland) was used in recording the surface pressure (π) – area (A) isotherms. Either pure water or 10 mM Tween 60 solution was used as the subphase. Monolayers were generated by careful spreading of 1mM chloroform-methanol (3:1) solution of lipids over the surface with a micro syringe. Solvent was allowed to evaporate for 20 min. After the generation and equilibration of the monolayer film the barriers were compressed at a rate of 5 mm/min²⁵. Hydrodynamic diameter (d_h), zeta potential (Z.P.) and polydispersity index (PDI) values were measured by a dynamic light scattering spectrometer

(Nano ZS 90, Malvern, UK). Morphology of the SLNs were studied by freeze fractured transmission electron microscope (FF-TEM, H-7650, Hitachi Science Systems Ltd., Japan). Differential scanning calorimetric studies were performed using DSC 1 STAR^c system (Mettler Toledo, Switzerland) with a scan rate of 2 °C min⁻¹. 40 µL sealed aluminium pan was used for DSC experiments. A pan containing dispersion medium (10 mM Tween 60) was used as reference¹⁴. Absorption and emission spectroscopic studies of curcumin loaded SLNs were made with UV-vis spectrophotometer (UVD-2950, LaboMed. Inc., USA) and bench-top spectrofluorimeter (Quantummaster-40, Photon Technology International, NJ, USA) respectively. Fluorescence anisotropy values were derived according to the following equation:²⁵

$$r = \frac{I_{VV} - G I_{VH}}{I_{VV} + 2G I_{VH}} \quad (1)$$

where, I_{VV} and I_{VH} are the fluorescence intensities and the subscripts indicate the position of the excitation and emission polarizer. G is the grating correction factor ($G = I_{HV}/I_{HH}$).

2.4. Entrapment efficiency and loading capacity studies

Percentage of curcumin entrapped in SLN was estimated by the method of centrifugation.²⁶ Entrapment efficiency (EE) and drug loading capacity (DL) of SLNs were calculated as:²⁶

$$EE\% = \frac{W_{TC} - W_{FC}}{W_{TC}} \times 100\% \quad (2)$$

$$DL\% = \frac{W_{TC} - W_{FC}}{W_{TC} - W_{FC} + W_{TL}} \times 100\% \quad (3)$$

where, W_{TC} , W_{FC} and W_{TL} represent the total amount of curcumin, free curcumin and total amount of lipid respectively.

2.5. *In vitro* drug release and release kinetic studies

Dialysis bag of 12 kDa (Sigma-Aldrich, USA) containing 10 mL of the curcumin loaded SLN formulation was suspended in 20 mL of release medium (aqueous 10 mM Tween 60)²⁷. The experiment was carried out under sink condition at room temperature with constant stirring. 5 µM curcumin in Tween 60 solution (10 mM) was used as control. The released curcumin was quantified colorimetrically.

2.6. Anti-bacterial activity

The cup-plate method²⁸ was adopted for the antibacterial activity studies of curcumin loaded SLNs. The studies were carried out using *Bacillus amyloliquefaciens* (gram positive, isolated from soil). Antibacterial activity was assessed by calculating the zone of inhibition.

All the experiments, unless otherwise stated, were carried out at 25 °C.

3. Results and discussion

3.1. Interfacial behavior of the monomolecular films

In order to assess the optimum lipid composition and to get an idea about the impact of FAs as well as curcumin, surface pressure (π) – area (A) isotherm of the lipids and curcumin in its pure form as well as in the form of mixtures were constructed. The lift-off area for SLC, TS, PA and curcumin appeared at 1.28, 0.63, 0.25 and 0.51 nm² molecule⁻¹ respectively (panel A of Fig. 1).

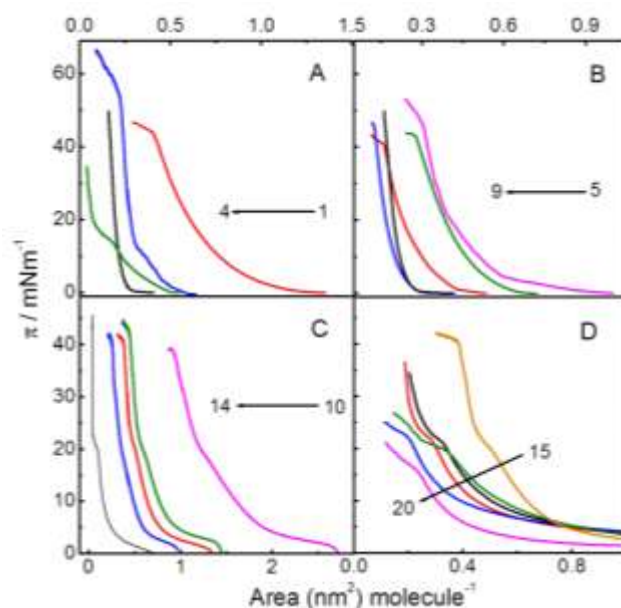


Figure 1. Surface pressure (π) – area (A) isotherm of SLC (1), TS (2), PA (3) and curcumin (4, panel A) and mixed monolayer of SLC+TS (1:1) and PA (panel B and C). Panel D describes the π -A isotherms of mixed monolayer of (SLC+TS+ PA, component 1) and curcumin(component 2). While pure water was used for A & B, 10 mM aqueous Tween 60 solution was used as subphase in C and D. Mole% of PA (B and C): 5 &10, 0; 6 &11, 10; 7 &12, 20; 9

&13, 80 and 8 &14, 100. Mole % of curcumin (Panel D): 15, 0;16, 80; 17, 40; 18, 50; 19, 60 and 20, 100. Temperature 25 °C.

The obtained results were found to be in good agreement with the literature values²⁹⁻³¹. In case of pseudo binary lipid mixtures, with water (panel B of Fig. 1) and Tween 60 solution (panel C of Fig.1) as subphase, isotherm of the pseudo binary mixed monolayer approached the isotherm of the pure FAs with increasing proportion of FA. Initially the surface pressure was zero when water was used as the subphase. However, in case of Tween 60 solution, being used as the subphase, the surface pressure increased to a finite value (2-3 mNm⁻¹). Inherent surface activity of Tween 60 was mainly responsible for the initial increase in surface pressure. No systematic variation in the collapse pressure with the progressive addition of FA in the surface pressure area isotherm of the lipid aggregated systems was observed in the present set of experiments. Presence of three structurally different lipids makes the orientation of the monolayer complicated at the closed pack state. Thus detail understanding on the variation in the collapse pressure with lipid composition and nature of the monolayer at the closed pack state, fluorescence microscopic analysis is warranted. Tween 60 enhanced both the lift-off area and initial surface pressure for all the systems, indicating the expansion of monolayer due to its hydrocarbon moiety³². In the closed pack state lipid molecules approaches the closest distance among them in the monolayer formed at the air water interface. The tristearin (TS) molecules also behave in the similar manner. In this situation the free movement of the hydrocarbon chains becomes restricted at the interface. It resembles the formation of the solid state in the closed pack situation. Further, increase in the surface pressure lead to desorption of the monolayer indicated by sudden drop in the surface pressure in the surface pressure area isotherm.

Compressibility modulus (C_s^{-1}) is defined as the reciprocal of film compressibility (C_s) which indicates the resistance of monolayer against compression²⁵. The state of a monolayer at air-solution interface depends on factors like hydrocarbon chain ordering and tilting of polar head group, etc²⁵. Compressibility modulus (C_s^{-1}) was calculated from the surface pressure (π)-% compressed area (%A) data using the following expression:²⁵

$$C_s^{-1} = -A \left(\frac{d\pi}{dA} \right)_T \quad (4)$$

Variation of C_s^{-1} with percentage of compressed area and surface pressure for some systems are shown as representative in Fig. 2.

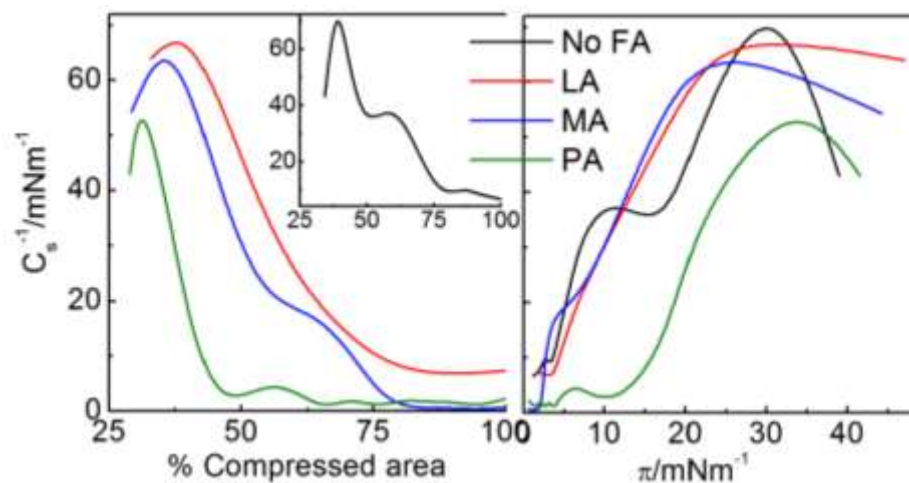


Figure 2. Dependence of compression moduli (C_s^{-1}) of (SLC+TS+FA, 2:2:1, M/M/M) monolayer with percentage of area compressed and surface pressure (π) at 25 °C. 10 mM aqueous Tween 60 solution was used as subphase. FAs are mentioned inside the figure.

C_s^{-1} values increased steadily and passed through maxima (left panel of Fig. 2). Multimodal nature in the C_s^{-1} vs. percentage of area compressed (% A) profile was observed for SLC+TS (1:1, M/M, inset of the left panel) mixed monolayer which disappeared with the addition of FA, indicating enhanced molecular association induced by added FA. Slope of the C_s^{-1} vs. % A curves increased with increasing FA chain length, which was due to increased molecular association through the hydrophobic interaction of the hydrocarbon chains of lipids and formation of condensed monolayer with FA³³. C_s^{-1} values increased with increasing surface pressure and passed through maxima, like the C_s^{-1} vs. % A curves (right panel of Fig. 2). Maximum C_s^{-1} (68.9 mNm⁻¹) was observed for SLC+TS (1:1, M/M) mixed monomolecular film. There occurred a decrease in the C_s^{-1} values with the incorporation of FA. Further reduction in C_s^{-1} was noted with increasing the FA chain length, which indicates associative interaction and formation of condensed/compact/rigid monolayer induced by FA³³.

For an ideal mixed monolayer, mean molecular area (A_{id}) can be expressed as:²⁵

$$A_{id} = x_1A_1 + x_2A_2 \quad (5)$$

where, x and A represent the mole fraction and area of the individual component. Excess molecular area (A_{ex}) was calculated as:²⁵

$$A_{ex} = A_{12} - A_{id} \quad (6)$$

where, A_{12} is the experimentally obtained mean molecular area of the mixed monolayer. In case of Tween 60 being used in the subphase, the obtained results were normalized with respect to the surface activity of Tween 60. Results for the PA comprising systems are shown in Fig. 3 as representative along with the changes in excess free energy of the mixing process.

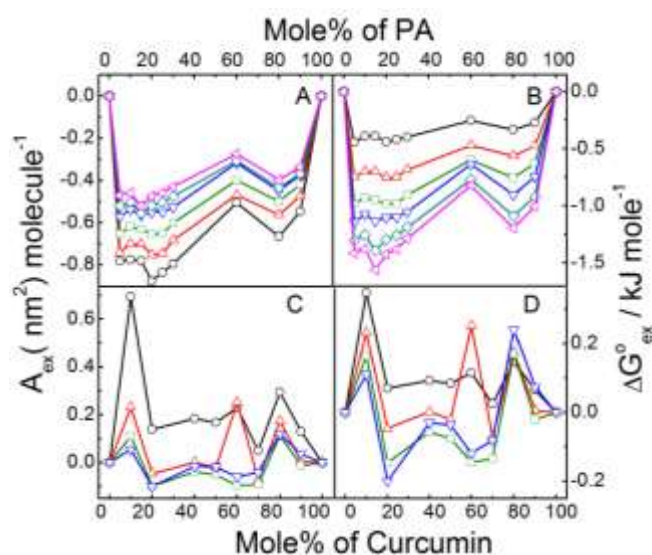


Figure. 3 Variation of excess molecular area (A_{ex}) and excess free energy change (ΔG_{ex}^0) with PA and curcumin mole%. For panel A, B: Component 1: SLC+TS (1:1, M/M), Component 2: PA. For panel C, D: Component 1: SLC+TS+PA (2:2:1, M/M/M), Component 2: curcumin. Surface pressure (mNm^{-1}): O, 5; Δ , 10; \square , 15; ∇ , 20; \diamond , 25 and \triangleleft , 30. Temperature: 25 °C

In case of FAs, observed negative deviation from ideality indicates associative interaction among the components.^{25, 30} Appearance of minima at 20 mole% FA indicates maximum association among the components. Additional stability for 20 mole% FA comprising systems was further established through the excess free energy (ΔG_{ex}^0) vs. composition profile (panel B of Fig. 3). Excess free energy of mixing was calculated using the following expression:^{25, 30}

$$\Delta G_{ex}^0 = \int_0^\pi [A - (x_1 A_1 + x_2 A_2)] d\pi \quad (7)$$

Decrease in the negative magnitude of A_{ex} and ΔG_{ex}^0 values were observed with the increase in FA amount above 20 mole% irrespective of the fatty acid chain length. On account of the obtained minima, 20 mole% FA was considered as optimum amount for further studies.

Miscibility of curcumin with the lipid mixtures (SLC+TS+FA, 2:2:1, M/M/M, considered as a single component) were also studied at the air-solution interface. Isotherms of PA comprising lipid mixture with varying mole% of curcumin have been shown in panel D of Fig. 1 as representatives. No systematic variation in the π -A isotherms with progressive addition of curcumin was observed. A_{ex} and ΔG_{ex}^0 vs. curcumin mole% profile are shown in the panel C and D of Fig. 3 respectively. Positive deviations in A_{ex} value indicated repulsive interaction between curcumin and the lipids. Inclusion of curcumin into the palisade layer, due to its rigid and amphiphilic nature, resulted in the expansion of monolayer.

3.2. Solution behavior of SLNs (DLS studies)

Hydrodynamic diameter (d_h), zeta potential (Z.P.) and polydispersity index (PDI) are the markers of physicochemical stability and performance of SLNs³⁴). Values of d_h and PDI at different time intervals have been shown in Fig. 4.

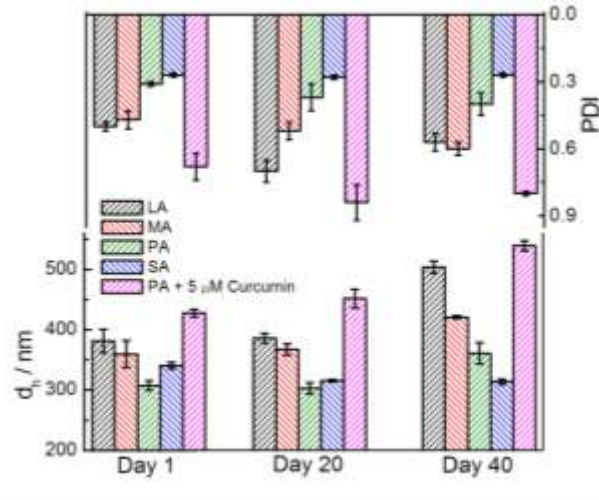


Figure 4. Variation in hydrodynamic diameter (d_h) and polydispersity index (PDI) with time for SLNs (SLC+TS+FA, 2:2:1, M/M/M). Samples were stored at 25 °C. FAs are mentioned inside the figure.

Size of SLNs were in the range 300-500 nm. Size distribution curve of some representative systems are given in the Fig. 5. Asymmetric unimodal size distribution (as shown in Fig. 5),

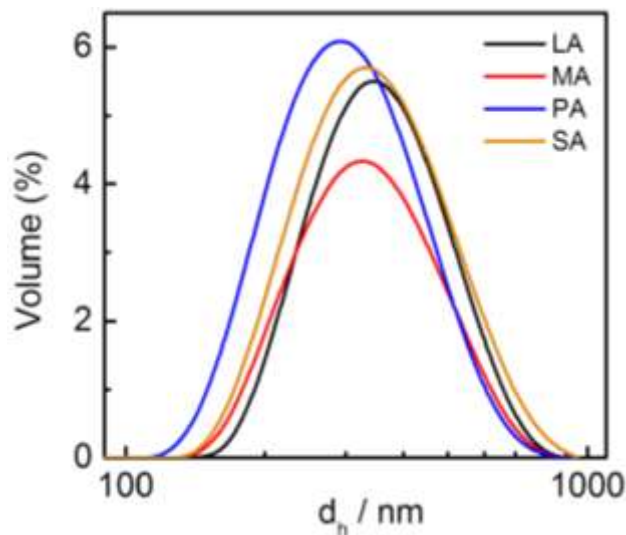


Figure 5. Hydrodynamic size (diameter, d_h) distribution of SLNs comprising different fatty acids. 1 mM SLN formulation of SLC+TS+FA (2:2:1, M/M/M) dispersed in 10 mM aqueous Tween 60 solution were studied. FAs are mentioned inside the figure. Temperature: 25 °C

indicates heterogeneity in the formation of SLNs. SLN formulations comprising of 5 – 30 mole% FA (with an increment of 5 mole%) were subjected for DLS studies. Although size of SLNs was not significantly dependent on FAs content. However, mild size constriction for 20 mole% FA

comprising systems were recorded. The observed reduction in size indicated the formation of well organized and compact packing of the lipid molecule at this composition. The monolayer experiments also supported the above observation. Obtained maximum associative interaction at 20 mole% FA comprising systems clearly indicated the formation of condensed system. Further, obtained maximum negative excess free energy (ΔG_{ex}^0) provided additional stability to 20 mole% FA comprising system. Results imply that 20 mole% FA was the optimum amount for imparting stability to SLNs.

An overall increase in the size of SLNs with time has been observed, except for SA. Size enhancement with time indicated ongoing crystalline modification during storage³⁵. Rate of crystalline modification towards more compact structures were found to be higher for LA and MA than PA and SA. The results could be rationalized on the basis of smaller hydrocarbon chain and low melting point of LA and MA, according to the proposition of Wong *et al*¹⁶. Higher d_h value in case of LA and MA indicates the formation of less organized SLNs. No significant change in size for PA and SA indicates the formation of more organized SLN due to the compatibility between PA/SA and the other lipids (in terms of hydrocarbon chain length). Such observations are in accordance with results obtained from monolayer studies (reduction in C_s^{-1} and increase in slope of C_s^{-1} vs. %A profile in case of PA and SA, compared to LA and MA). All the formulations became unstable after 45 days, as revealed through drastic size enhancement. Curcumin loaded SLNs followed almost similar size–time profile as that of the blank SLNs that led to conclude that curcumin was in the palisade layer and did not interfere with the crystalline modification undergoing in the core of SLN matrices^{36, 37}. Increased PDI value with added curcumin suggests its irregular surface accumulation. No marked effect of curcumin concentration on PDI value was observed.

Zeta potential (Z.P.) is a direct measure of the surface charge which regulates the physical stability of SLN by preventing particle aggregation during storage. For the studied systems, Z.P. values were in the range -10 to -20 mV. Steric stabilization associated with Tween 60 was clearly reflected by the suppressed Z.P. values³⁸⁻⁴⁰. Irregular variation in Z.P. with increasing FA concentration was an ambiguity, which needs further investigation. Curcumin reduced the negative Z.P. value of SLNs. Z.P. value did not change systematically with curcumin concentration. Z.P. for the curcumin loaded systems were in the range of -7 to -9 mV. Reduction in the magnitude of negative Z.P. accounts for the location of curcumin in the palisade layer of

SLN. Presence of curcumin onto the interface resulted in a non polar environment which suppressed the FA dissociation³⁸.

3.3 Morphological Studies

Morphology of the SLNs were investigated by freeze fractured TEM (FF-TEM) technique. FF-TEM images of SLNs with PA in the absence and presence of curcumin have been shown in Fig. 6 as representatives.

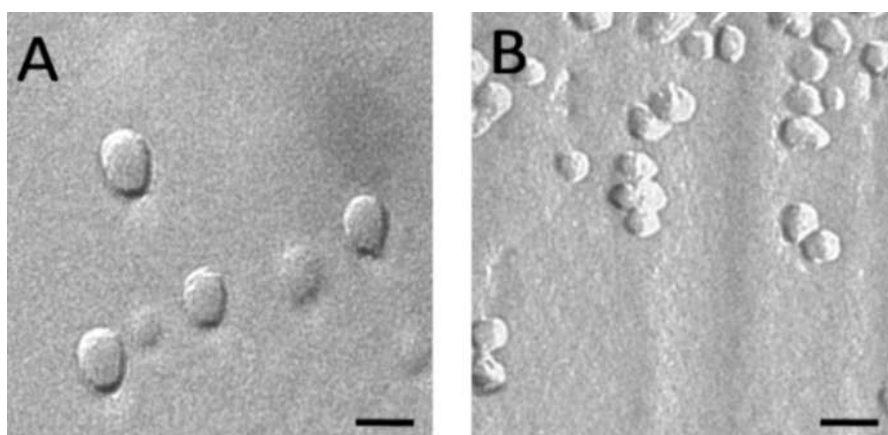


Figure 6. FF-TEM images of SLN (SLC+TS+ PA, 2:2:1, M/M/M) in the absence (A) and presence (B) of curcumin. Scale bar: 500 nm.

SLNs were nearly spherical in shape with surface imperfections and size ranged between 200 - 300 nm, comparable with the DLS data. Uneven surface morphology of the curcumin loaded SLNs were observed in comparison to the SLN without curcumin from FF-TEM studies. The observed unevenness of the surface indicated the presence of curcumin in the palisade layer of SLNs. Also curcumin promoted the formation of the aggregated structures between two or more SLNs whereby curcumin acted as ‘adhesive/glue’ between two SLN particles. Increase in the hydrodynamic diameter as well as PDI value for the curcumin loaded SLNs also indicated the existence of aggregated structured formed.

3.4 Differential scanning calorimetric (DSC) studies

Effect of FAs and curcumin on SLNs were also investigated by DSC studies. Results have been summarized in table 1.

Table 1. Phase transition temperature (T_m), peak width (ΔT), change in enthalpy (ΔH) and heat capacity (ΔC_p) of SLNs (SLC+TS+FA).

	Mole% of FA	$T_m/^\circ\text{C}$	$\Delta T/^\circ\text{C}$	$(-)\Delta H/ \text{k cal.mol}^{-1}$	$\Delta C_p/ \text{kcal.mol}^{-1}\text{C}^{-1}$
LA	0	29.02	6.86	32.84	4.78
	15	27.82	6.79	31.26	4.60
	20	27.89	7.41	29.84	4.02
	25	26.62	10.01	25.55	2.55
MA	0	29.02	6.86	32.84	4.78
	15	27.11	6.67	14.08	2.11
	20	27.53	6.97	18.19	2.60
	25	26.66	8.81	21.24	2.41
PA	0	29.02	6.86	32.84	4.78
	15	28.5	6.41	20.25	3.16
	20	27.74	7.13	13.06	1.83
	25	26.92	10.60	16.89	1.59
SA	0	29.02	6.86	32.84	4.78
	15	28.79	6.92	26.04	3.76
	20	30.59	3.47	1.31	0.37
	25	30.69	3.45	2.51	0.73

Concentration of the SLNs were fixed at 5mM. All the DSC studies were performed on day1. Scan rate: 2°C min^{-1} .

While blank SLNs with 15, 20 and 25 mole% of FA were studied, SLNs with 20 mole% FA were used for curcumin loaded systems. In all the cases, while the endothermic heating curves were broader, the cooling curves were narrower and distinct (Fig. 7).

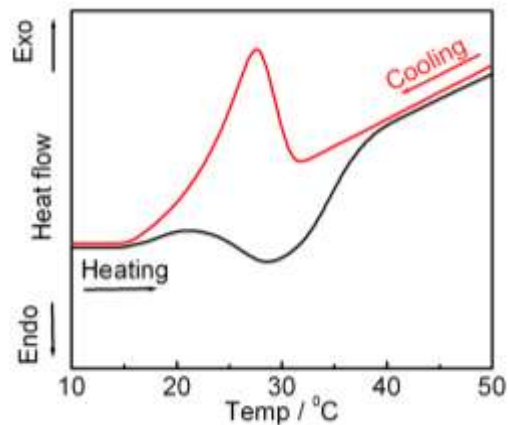


Figure 7. DSC thermogram of a 5 mM SLN formulation (SLC+TS+PA, 2:2:1, M/M/M). Scan rate: 2 °C / min.

Similar to the liquid crystalline systems, temperature of maximum heat flow in the cooling scan appeared $\sim 2 - 3$ °C below the same detected in the heating scan. The cooling thermograms were, therefore, used for further evaluation of thermal parameters like temperature of maximum heat flow (T_m), difference between the onset and end set temperature of phase transition process (ΔT), change in enthalpy (ΔH) and heat capacity (ΔC_p)^{14, 25}. DSC cooling thermograms of SLNs with different FAs have been shown in Fig. 8.

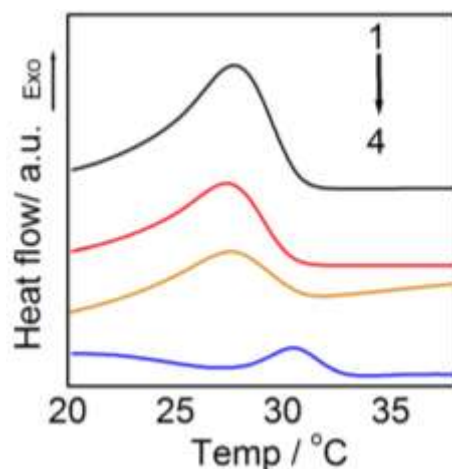


Figure 8. DSC cooling thermograms of 5mM SLNs (SLC+TS+FA, 2:2:1, M/M/M, stabilized by 10 mM aqueous Tween 60) with different fatty acids (1, LA; 2, MA; 3, PA and 4, SA). Scan rate: 2 °C /min

T_m values appeared in the range of 26-30 °C. A significant decrease in the T_m value for SLNs, compared to the bulk mixture of lipids, were due to the decreased size of the aggregates according to Thomson proposition^{20, 41}. Reduction in T_m was due to the multicrystallinity in SLNs as lipid blends and Tween 60 were used in the formulation. Modified SLNs are prepared mainly by using lipid blend containing two or three structurally different lipids. The individual lipid molecules exist in their specific liquid crystalline arrangement. When used in the preparation of SLN, their original liquid crystalline arrangements are not totally destroyed but get influenced by the other constituent lipids. For this reason a modification in liquid crystalline arrangement is observed with enhanced disorderedness in the modified solid lipid nanoparticle. Fig. 8 describes the effect of FA chain length on T_m for the systems with 20 mole% FA. The system without any FA was also studied and it was found that the transition temperature (29.02 °C) was suppressed by FA through the generation of multicrystalline structure. While the T_m values did not appreciably change for LA, MA and PA, however, for SA it increased to 30 °C (~28 °C for the others). Well organized compact molecular packing due to similarity in hydrocarbon chain among TS and SA resulted in the up shift of the melting temperature. Significant decrease in the difference between the onset and end set temperature of phase transition process (ΔT) for SA comprising systems was noticed whereas for all other systems increasing ΔT value indicated enhanced multicrystallinity. No systematic variation in ΔT value with FA chain length was observed.

Both the ΔH and ΔC_p values decreased with increasing mole% of FA, the effects were more prominent with the higher FAs¹⁶. Small chain FAs have the capability to melt to higher extent, hence for those systems, higher amount of thermal energy would be required for phase transition. No major change in the thermal behavior of SLN with varying proportion of curcumin (2.5 to 7.5 μM) was noted, indicating its insignificant effect on the thermal behaviour of SLNs because of its location in the interfacial region of SLNs.

In the present set of work it was found that, stearic acid (SA) comprising SLNs were more compact in nature in comparison to the SLNs comprising other fatty acids. The similarity in the hydrocarbon chain length between tristearin (TS) and stearic acid (SA) lead to the formation of compact molecular packing in SLNs. Lauric (LA), myristic (MA) and palmitic acid (PA) were found to produce SLNs having more multicrystallinity. The structural mismatch between the lipid components and the fatty acids was mainly responsible for this phenomenon. The observation has the following facets: in case of compact SLN (comprising symmetric hydrocarbon entities), enhanced stability are resulted; on the other hand systems with dissymmetric components will have not that high stability. However, a stable system is not suitable for the loading of different kinds of hydrophobic drugs. The DSC studies thus could help in identifying the optimum formulation as drug delivery systems.

3.5. Spectroscopic studies

UV-visible absorption spectra of curcumin were recorded in different solvents as well as the same loaded in SLNs (panel A, Fig. 9).

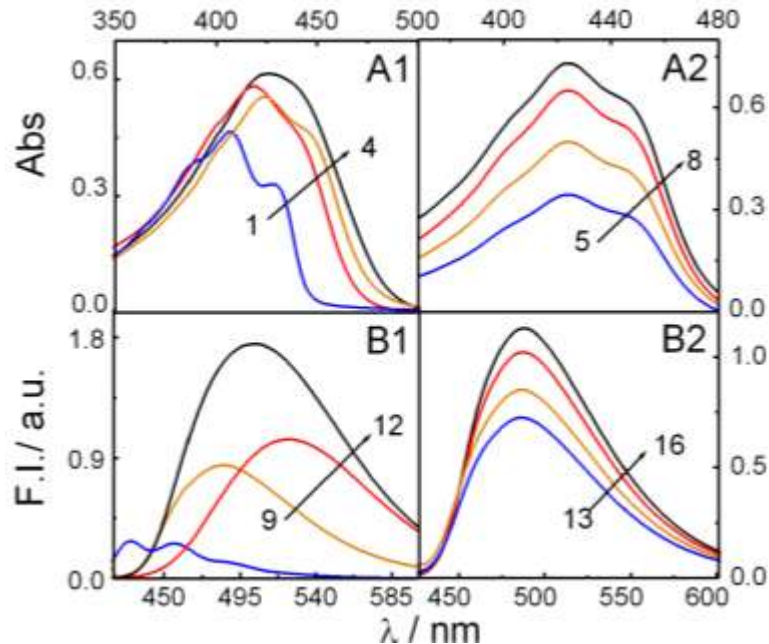


Figure 9. Absorption (A) and emission (B) spectra of 5 μ M curcumin in different solvents (A1, B1) and SLNs (SLC+TS+FA, 2:2:1, M/M/M) (A2, B2) at 25 $^{\circ}$ C. Systems: 1&9, n-hexane; 2& 10, aqueous 10 mM Tween 60; 3& 12, acetonitrile; 4 & 11, ethanol; 5 & 13, SA; 6 & 14, PA; 7 & 15, MA and 8 & 16, LA. $\lambda_{\text{ex}}=419$ nm.

Appearance of broad spectra with shoulders on the either side of the maxima (λ_{max}) indicate the existence of more than one tautomeric form (keto-enol tautomerism) of curcumin⁴². The shoulders were less prominent in solvents of higher polarity⁴³. While a red shift in the λ_{max} value with increasing solvent polarity was noticed for aprotic solvents, in case of protic solvents, there occurred blue shift in λ_{max} value with increasing solvent polarity (Fig.10)

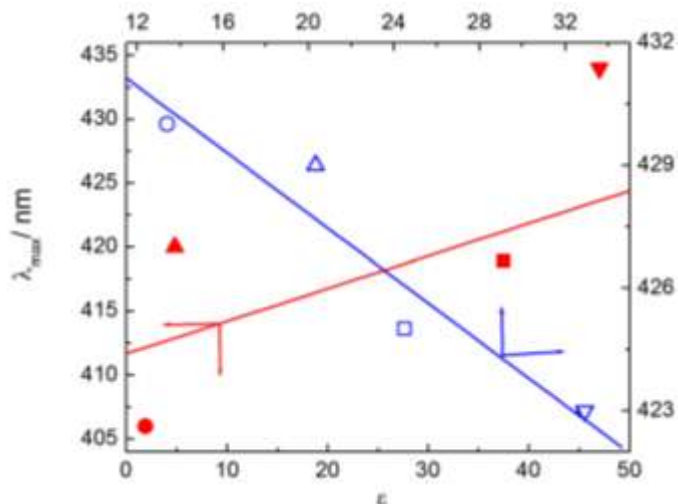


Figure 10. Dependence of the absorption maxima (λ_{\max}) of curcumin on dielectric constant (ϵ) of the medium at 25 °C. Red and the blue line correspond to the aprotic and protic solvents respectively. Solvents: ●, hexane; ▲, chloroform; ■, acetonitrile; ▼, DMSO; ○, pentanol, ▲, propanol; □, ethanol and ▽, methanol. 5 μ M curcumin was used in recording the spectra.

which were in conformity with the earlier observation⁴³. In case of SLNs, the λ_{\max} values appeared at 422 nm. Insignificant change in the λ_{\max} values with FA chain length variation further suggests the location of curcumin on the palisade layer of the SLNs. A linear variation in the absorption maxima of curcumin with dielectric constant of the medium was observed (Fig. 10). From such profile one can predict the state of polarity of curcumin loaded in SLN¹⁴. Dielectric constant, experienced by curcumin loaded in the SLNs, was found to be ~ 33 (close to methanol) when compared to the shift in polar protic solvents. This suggests the localization of curcumin in more hydrophilic environment, herein the palisade layer of SLNs¹⁴.

Similar to the absorption spectra, a solvent dependent shift in the emission maximum was recorded (panel B, Fig. 9)⁴².

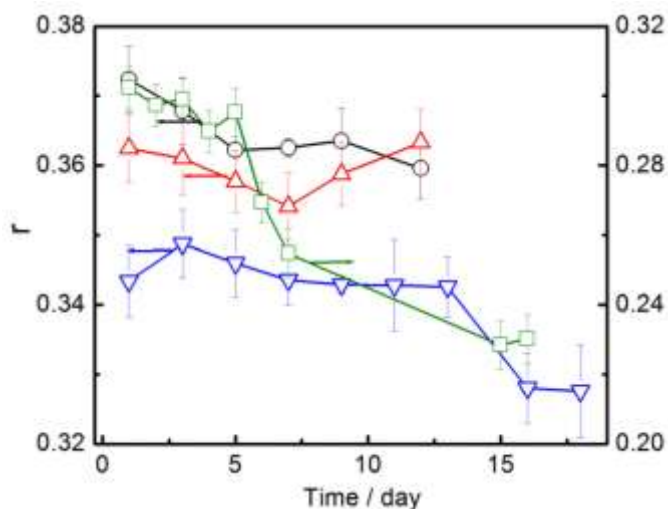


Figure 11. Variation in the fluorescence anisotropy (r) with time for curcumin loaded SLNs comprising four different fatty acids. Fatty acids: O, LA; Δ , MA; \square , PA and ∇ , SA. The concentration of curcumin was 5 μM . Excitation wavelength and emission wavelength were set at 419 and 458 nm respectively. Temperature, 25 $^{\circ}\text{C}$.

Unlike the absorption spectra, fluorescence spectra of curcumin loaded SLN were more symmetric in nature with the maximum appearing at 487 nm, being independent of FA chain length. Emission spectra of curcumin in most of the solvents were unimodal excepting n-hexane (structured bands)⁴⁴. No significant difference between the emission spectra of curcumin in Tween 60 and in the prepared formulations strengthened the fact that the molecularly dispersed curcumin molecules were in contact with continuous medium of the SLNs as they got accumulated over the surface. Fluorescence intensity decreased with increasing FA chain length. Decrease in fluorescence anisotropy value with time (Fig. 11 clearly indicates desorption of curcumin from SLN surface⁴⁵⁻⁴⁷).

3.6. Curcumin entrapment efficiency (EE) and loading (DL) capacity studies

EE and DL capacity of the SLNs, with respect to curcumin as the model drug, have proportional relationship with the therapeutic efficacy. Results on the EE and DL values have been graphically shown in Fig. 12 and Table 2. EE decreased with increasing FA chain length; while for LA it was 73.4%, for SA the value went down to 43% (Fig. 12 left panel).

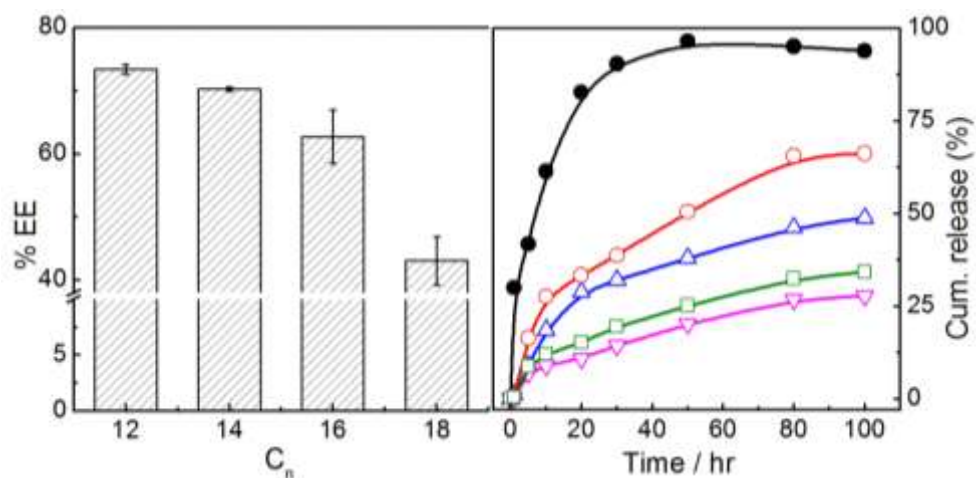


Figure 12. Dependence of entrapment efficiency (EE) and *in vitro* release profile of curcumin loaded SLN (SLC+TS+FA, 2:2:1, M/M/M) on the fatty acid chain length (C_n) at 25 °C. Systems for right panel: ●, control; ○, LA; △, MA; □, PA and ▽, SA.

Decrease in the DL value was also noted with increasing FA chain length (table 2). Curcumin, being amphiphilic in nature is expected to be located in the SLN surface to higher extent than a hydrophobic drug, which resides in the core of SLNs²⁰. LA and MA, being more fluidic than PA and SA, can exert greater flexibility for which the corresponding SLN can accommodate larger number drug molecules.

3.7. *In vitro* release studies of curcumin

In vitro release of curcumin from the SLNs were studied by dialysis bag method²⁷. Parallel experiment was performed with curcumin dissolved in aqueous Tween 60 solution as control. Obtained release profiles have been graphically presented in the right panel of Fig. 12. SLNs sustained the release process of curcumin compared to the diffusion of free curcumin (control, dissolved only in 10 mM Tween 60). A biphasic release pattern was obtained; sustained release profile followed an initial burst release^{20, 22}. Release process of all the systems were studied up to 100 h. There occurred an initial burst release of 20-25% curcumin within 9-10 h, which was due to the weakly adsorbed curcumin. Kinetic parameters, obtained by fitting the curcumin release profile in different release models, are shown in table 2. DD Solver 1.0, an Add-In program, was used in evaluating the release kinetics parameters. Comparison was made among the pseudo first order, zero order, Korsmeyer-Peppas, Higuchi and Weibull model (table 2). Korsmeyer-Peppas release kinetic model, the best fit model,⁴⁸ describes the controlled and sustained release of

curcumin. Values of the release exponent (n) were also recorded for Korsmeyer-Peppas release model which was found to be ≤ 0.5 , which indicate that the release of curcumin was subjugated by classical Fick diffusion formalism. A decrease in the rate constant was observed with increasing FA chain length. Less ordered lipid matrix structure and less organized nature for LA and MA resulted in faster elution because of non-systematic binding²⁰. PA and SA comprising systems restricted desorption of curcumin for its more organized structure and compact molecular organization. Due to the more organized nature and compact molecular packing, SA comprising SLNs were able to bind curcumin systematically and firmly on the palisade layer of SLN. Hence the release of curcumin was sustained in case of SA comprising systems.

Table 2 Release kinetics of curcumin from SLN containing different FAs.

Curcumin loaded SLN formulations containing different FA	First order		Zero order		Weibull		Korsmeyer-Peppas			Higuchi		Drug loading capacity (%)
	k_1/ h^{-1}	R^2	$k_0/ mol\ lit^{-1}.h^{-1}$	R^2	k_w/ h^{-1}	R^2	k_k/ h^{-n}	R^2	n	$k_h/ h^{-0.5}$	R^2	
LA	0.014	0.866	0.827	0.677	0.534	0.981	8.736	0.988	0.4	7.101	0.976	0.054
MA	0.008	0.869	0.557	0.810	0.396	0.955	4.822	0.993	0.5	5.103	0.954	0.046
PA	0.005	0.736	1.000	0.884	0.512	0.994	4.206	0.992	0.4	3.564	0.989	0.034
SA	0.004	0.845	0.354	0.781	0.565	0.987	2.669	0.988	0.5	2.830	0.988	0.014

Concentration of SLN (SLC+TS+FA, 2:2:1): 1 mM, and curcumin: 0.5 μ M.

3.8. Anti-bacterial activity studies

Curcumin loaded SLNs showed significant antibacterial activities towards *Bacillus amyloliquefaciens* (gram positive, isolated from soil). SLNs without curcumin were non responsive. Obtained distinct zone of inhibition (24 h of incubation) for curcumin loaded SLNs are shown in Fig. 13.

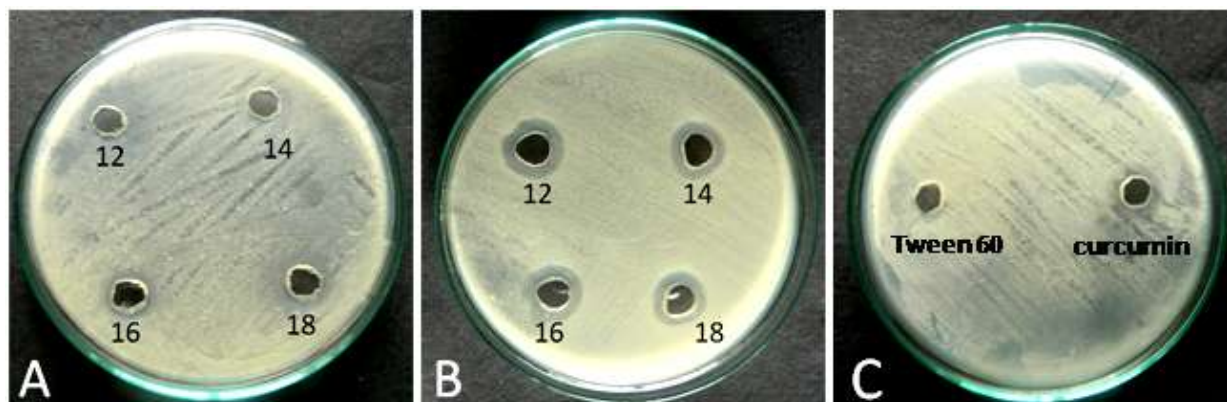


Figure 13. Inhibitory effect of curcumin loaded SLNs (B) on the growth of *Bacillus amyloliquefaciens*. SLNs without curcumin were used as control (A). Panel C represent the activity of curcumin alone using Tween 60 as control. Fatty acid chain lengths are mentioned inside the figure.

Nearly 22 - 28% (LA, 22%; MA, 25%; PA, 25% and SA, 28%) of inhibition zone were recorded, which were independent of FA chain length. Antibacterial activity was not that significant for curcumin in Tween 60, as shown in panel C. Thus, curcumin loaded SLNs could be considered as potential antibacterial drug delivery agents. However further studies using other pathogenic bacterial strains are required to explore the broad spectrum antibacterial activity of such formulations. Besides, some *in vivo* studies using other human cell lines are also warranted, being considered as the future perspectives. It is difficult to correlate the release data with the inhibition zone obtained in this approach. For the quantitative correlation between the drug release and *in vivo* studies are warranted and are endeavoring for this kind of study.

4. Conclusion

Langmuir monolayer studies of lipids with and without curcumin were performed to understand the interaction between the lipids and the drug. Monolayer studies on the components led to conclude that 20 mole% FAs provided optimum stability. Curcumin resulted in the expansion of lipid monolayer. SLNs with FAs of different chain length and molar ratio were formulated in combination with SLC and TS. Curcumin as a model drug was also assimilated in the preparation. SLN formulations were found to be stable up to 45 days. Although the zeta potential values were low, however the SLNs were stable due to the combined electrostatic and steric stabilization induced by the dissociated FA and the hydrophilic polyoxyethylene moiety of Tween 60 respectively. Combined DLS, DSC and spectroscopic investigations confirmed the location of curcumin in the palisade layer of SLNs. SA exhibited highest crystallinity in the SLNs. Due to the unorganized nature and structural mismatch with TS, LA comprising systems exhibited higher drug incorporation and loading capacities as well as faster release of the entrapped drug. On the contrary, structural similarity between SA and TS rendered such combinations to become more compact in nature for which lower entrapment and slower release of curcumin from such systems were recorded. Curcumin loaded SLNs showed antibacterial activity. Further information on the crystallinity (by XRD) and *in vivo* activities are warranted towards better appreciation of structure – activity relationship of the SLNs, being considered as future perspectives.

References

References are given in BIBLIOGRAPHY under references for CHAPTER 1 (pp.152-154).